



Influence of Mn content on the magnetic properties of the hexagonal Mn (Co,Ge)₂ phase

Daniel Hedlund^a, Simon Rosenqvist Larsen^b, Martin Sahlberg^b, Peter Svedlindh^a, Vitalii Shtender^{b,*}

^a Department of Materials Science and Engineering, Uppsala University, Box 35, 75103 Uppsala, Sweden

^b Department of Chemistry – Ångström Laboratory, Uppsala University, Box 538, 75121 Uppsala, Sweden

ARTICLE INFO

Keywords:

Permanent magnets
Intermetallic compound
Synthesis
Magnetocaloric properties
Crystal structure

ABSTRACT

Herein, we report on the effect of Mn content on the magnetic properties of the hexagonal Mn(Co,Ge)₂ with composition Mn_{36+x}Co_{49-x}Ge₁₅. This compound was previously described as Mn₂Co₃Ge (MgZn₂-type structure), but later as Mn(Co,Ge)₂ with its own structure type, all samples in this work follow the same superstructure model. Samples were synthesized by induction melting, the crystal structures were evaluated using a combination of X-ray diffraction together with scanning electron microscopy equipped and an energy dispersive X-ray spectroscopy detector. The Curie temperature (T_C) is shifted towards lower temperature as the Mn content is increased. On the other hand, the spin reorientation temperature (T_{SRT}) increases and the magnetic moment decreases as the Mn content is increased. The magnetocaloric properties were investigated for the $x = 1$ alloy, Mn₃₇Co₄₈Ge₁₅. It was found that the isothermal entropy change is 2 J kg⁻¹ K⁻¹ at room temperature for an applied field of 5 T.

Index Terms: In a data-mining survey of new permanent magnets from a combination of two 3d elements together with an additional element the material Mn₂Co₃Ge (MCG) was highlighted [1]. The crystal structure of Mn₂Co₃Ge has been described in [2] as either an ordered Mg₂Cu₃Si- or disordered MgZn₂-type structure, both hexagonal crystal systems with $P6_3/mmc$ space group [2]. In previous work [1], we found that the structure is best described as a disordered MgZn₂ structure with intermixing of Co and Ge. Moreover, using neutron powder diffraction additional peaks not visible from X-ray diffraction were found [3], which were assigned to a supercell where a and b were doubled, while intermixing of Co/Ge was still present [3]. In Fig. 1, we show a comparison of the two structures of MCG with the small and big cells.

Ab-initio calculations (at 0 K) predicted the material to be fully ordered and to have a saturation polarization of 1.71 T, a uniaxial magnetocrystalline anisotropy constant of 1.44 MJ/m³ and a Curie temperature (T_C) of 700 K [1]. Experimentally, it was shown that these values are somewhat overestimated yielding a saturation polarization of 0.86 T at 10 K, a uniaxial magnetocrystalline anisotropy constant of 1.18 MJ/m³ and a T_C of 359 K. These discrepancies were explained based on the order/disorder factor of Co/Ge. Results of calculations taking into account thermally induced spin-fluctuations yields better agreement

between theoretical and experimental results [3]. Moreover, another interesting feature of MCG was highlighted, that of a spin reorientation (T_{SRT}) from uniaxial magnetic anisotropy to an easy cone magnetic state, which later was described as an incommensurate antiferromagnetic structure [3]. A spin reorientation temperature has also been found for other Mn–Co–Ge phases, for details see appendix H in [1].

This study is motivated by the Mn₂Co₃Ge compound being proposed as a rare-earth free permanent magnet material by Vishina *et al.* [1]. Initial trials revealed the magnetic Heusler phase MnCo₂Ge [4] as being the main competing phase in the phase diagram. Several attempts have been made to produce MnCo₂Ge-free samples by arc melting and excess of Mn (1–10 wt%). With this approach a new Mn₁₄(Co,Ge)₂₃ compound was found [5], but a high purity sample of the Mn₂Co₃Ge compound could not be achieved. The final Mn₃₆Co₄₉Ge₁₅ composition was found with the help of scanning electron microscopy (SEM) equipped with energy dispersive X-ray spectroscopy (EDS). A single phase sample has been synthesized by induction melting [3]. It was noticed that from alloy to alloy the cell parameters of the main phase change quite a lot, suggesting some homogeneity region. In this spirit, the current investigation was initiated to study the effect of the composition of the target compound on the magnetic properties.

* Corresponding author.

E-mail address: vitalii.shtender@angstrom.uu.se (V. Shtender).

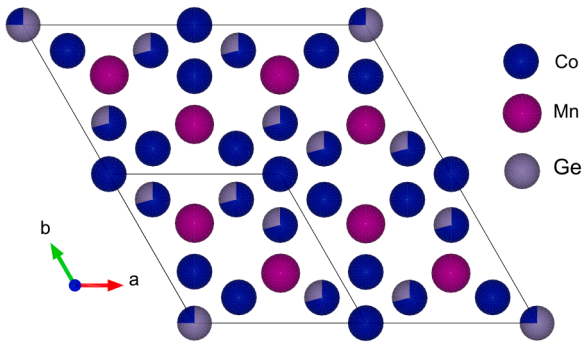


Fig. 1. Crystal structure of $\text{Mn}(\text{Co,Ge})_2$ -type vs. MnZn_2 -type viewed along the crystallographic c -axis. The purple atoms are Mn, while the blue and gray are Co and Ge, respectively. The black borders show the large and small unit cell. (For interpretation of the references to colour in this figure legend, the reader is referred to the web version of this article.)

In this paper, we report on the effect of the Mn content on the magnetic properties for $\text{Mn}_{36+x}\text{Co}_{49-x}\text{Ge}_{15}$ ($0 \leq x \leq 4$), adopting the same crystal structure with the super cell as was found from neutron powder diffraction results of $\text{Mn}(\text{Co,Ge})_2$ ($\text{Mn}_{36}\text{Co}_{49}\text{Ge}_{15}$) [3]. We highlight the properties of changing the Mn content, as this changes not only structural parameters of the compound but also physical properties such as T_C and T_{SRT} . The main findings in our survey are that increasing the Mn content of $\text{Mn}_{36+x}\text{Co}_{49-x}\text{Ge}_{15}$ reduces the values of T_C and the magnetization, while the value of T_{SRT} increases. In addition to this, we evaluate the magnetocaloric properties of $\text{Mn}_{37}\text{Co}_{48}\text{Ge}_{15}$ as its T_C is close to room temperature. The previously published $\text{Mn}_{34}\text{Co}_{52}\text{Ge}_{14}$ [1] is taken as a comparison in the discussion.

Samples of $\text{Mn}_{36+x}\text{Co}_{49-x}\text{Ge}_{15}$ ($x = 0, 1, 2$ and 4) were synthesized by melting Co (99.9%), Mn (99.999%) and Ge (99.999%) together in an induction furnace in Al_2O_3 crucibles and under Ar (99.999%) atmosphere. A 3wt% excess of Mn was used to compensate its evaporation during high temperature melting. The resulting ingots weighing 6 g were placed in Al_2O_3 crucibles, sealed in stainless steel tubes under Ar atmosphere and annealed at 1073 K for 2 weeks after which they were quenched in cold water. In the end, samples were manually ground and powders taken for further analysis.

The phase content of the samples was checked with X-ray powder diffraction (XRPD) and scanning electron microscopy (SEM) equipped with an energy dispersive X-ray spectroscopy (EDS) detector. XRPD patterns were collected using a Bruker D8 Advance with $\text{Cu-K}\alpha$ radiation at room temperature. The Rietveld method implemented in the FullProf program was used for analysis of the diffraction data [6]. The crystal structure was also studied using the single crystal method to corroborate the superstructure model from [3]. A Bruker D8 single-crystal X-ray diffractometer with $\text{Mo K}\alpha$ radiation was utilized to collect single crystal X-ray diffraction (SCXRD) intensities at room temperature. The CrystalisPro software was used to differentiate the weak superlattice peaks and further data reduction with numerical absorption correction. The structure solution was performed using the Superflip method and subsequent refinements were carried out using JANA2020.

Magnetization versus field and temperature measurements were performed using a Quantum Design MPMS XL system. Isothermal magnetization curves were recorded at several temperatures in applied magnetic fields up to 5T. The temperature dependent magnetization was measured between 10 K and 390 K in an applied magnetic field of 0.01T. The isothermal magnetic entropy change (ΔS_M) was estimated by using Maxwell's relation:

$$\Delta S_M(T, H_f) = \mu_0 \int_0^{H_f} \left[\frac{\partial M(H, T)}{\partial T} \right]_H dH,$$

where μ_0 is the vacuum permeability, T is the temperature and H_f is the final magnetic field. The isothermal magnetic entropy change was numerically calculated using the trapezoid rule as:

$$\Delta S_M(T, H_f) = \mu_0 \sum_i \frac{M(T + \Delta T, i \cdot \Delta H) - M(T - \Delta T, i \cdot \Delta H)}{2\Delta T} \times \Delta H$$

where $0 \leq i \cdot \Delta H \leq H_f$, ΔH is the magnetic field increment used in the isothermal magnetization measurements and ΔT is the temperature difference between neighbouring magnetic isotherms.

Now, we start describing the results obtained from X-ray diffraction for $\text{Mn}_{36+x}\text{Co}_{49-x}\text{Ge}_{15}$. This is followed by a discussion of the effect of Mn content on the magnetic properties and the magnetocaloric effect of $\text{Mn}_{37}\text{Co}_{48}\text{Ge}_{15}$, which has a magnetic ordering temperature close to room temperature.

Using SEM/EDS it was established that contrary to the desired $\text{Mn}_{33.33}\text{Co}_{50}\text{Ge}_{16.67}$ composition, single phase samples of the Laves phase exists with composition $\text{Mn}_{36}\text{Co}_{49}\text{Ge}_{15}$. A homogeneity region for $\text{Mn}_{36}\text{Co}_{49}\text{Ge}_{15}$ along the 15at% of Ge was found substituting Mn with Co (Fig. 2a). Taking literature data into account, we see that all homogeneity regions for ternary compounds in the Mn–Co–Ge system have a constant Ge:Mn/Co ratio.

Four $\text{Mn}_{36+x}\text{Co}_{49-x}\text{Ge}_{15}$ ($0 \leq x \leq 4$) single phase alloys have been synthesized in the present work, Table 1. Substituting Mn for Co shifts the XRD peaks to lower 2θ values, Fig. 2b(inset), which indicates increasing cell parameters in accordance with the atomic radii of Mn and Co ($r_{\text{Mn}} = 1.27 \text{ \AA}$, $r_{\text{Co}} = 1.25 \text{ \AA}$ [7]). As it was mentioned before, $\text{Mn}_{36}\text{Co}_{49}\text{Ge}_{15}$ has the $\text{Mn}(\text{Co,Ge})_2$ -type structure and all other Mn enriched compositions behave similarly, Fig. 2c. To resolve the superlattice peak, an extra-long exposure time was used for a short region of the XRPD 2θ -scan (intensities from single crystal can be found in [3]). Cell parameters from XRPD and SCXRD data are shown in Table 1. Rietveld refinements of the XRPD data of $\text{Mn}_{36}\text{Co}_{49}\text{Ge}_{15}$ are presented in Fig. 2d.

Atomic positions and Mn/Co/Ge intermixing have been precisely determined in previous related work [3] for $\text{Mn}_{36}\text{Co}_{49}\text{Ge}_{15}$ using neutron powder diffraction data. It was shown that Co/Ge occupy 12j and 2a positions while 6g is occupied by Mn/Co. Four other positions are singly occupied: Mn (4f and 12k) and Co (6h1 and 6h2). The SCXRD study revealed the same phenomenon of intermixing, except Mn/Co since it is very difficult to differentiate these two closely related atoms using X-ray diffraction. In the present study the ratio Mn/Co has been varied, and as a result changes in the occupation of the 6g position are expected. However, the situation with the 2a and 12j positions is unclear - it might be that Mn replaces Co there as well. To resolve this issue, one would need neutron diffraction (NPD) measurements for all samples.

Field cooled magnetization results are shown in Fig. 3a. The overall behavior is similar to the previously studied $\text{Mn}_{34}\text{Co}_{52}\text{Ge}_{14}$ (with 4.6 wt % of MnCo impurity) [1] and $\text{Mn}_{36}\text{Co}_{49}\text{Ge}_{15}$ [3] compounds.

The observed temperature dependent features are paramagnetic to ferromagnetic and spin reorientation transitions. In a previous study [1], the Curie-Weiss law was used, however, for the samples in this study there is a large deviation from the Curie-Weiss behavior (not shown in figure). Instead, the inflection point of the magnetization versus temperature curve was used to determine T_C . Increasing the Mn content decreases T_C from 330 K ($x = 0$) to 229 K ($x = 4$), while T_{SRT} increases from 187 K ($x = 0$) to 210 K ($x = 4$); the results are summarized in Table 1 together with the crystallographic parameters. The reference sample has a slightly lower Ge content than the samples presented in this work, but it is evident that increasing the Mn content shifts T_C to lower temperature and T_{SRT} to higher temperature. A peculiar situation may occur if $T_{SRT} = T_C$; extrapolation of $T_{SRT}(x)$ and $T_C(x)$ indicates a crossing at $x \approx 4.25$, which is outside the homogeneity range of the system. However, measurements on a sample with $x \approx 4.25$ (not seen in figure) containing only 3wt% of the desired hexagonal phase indicates $T_{SRT} \neq T_C$.

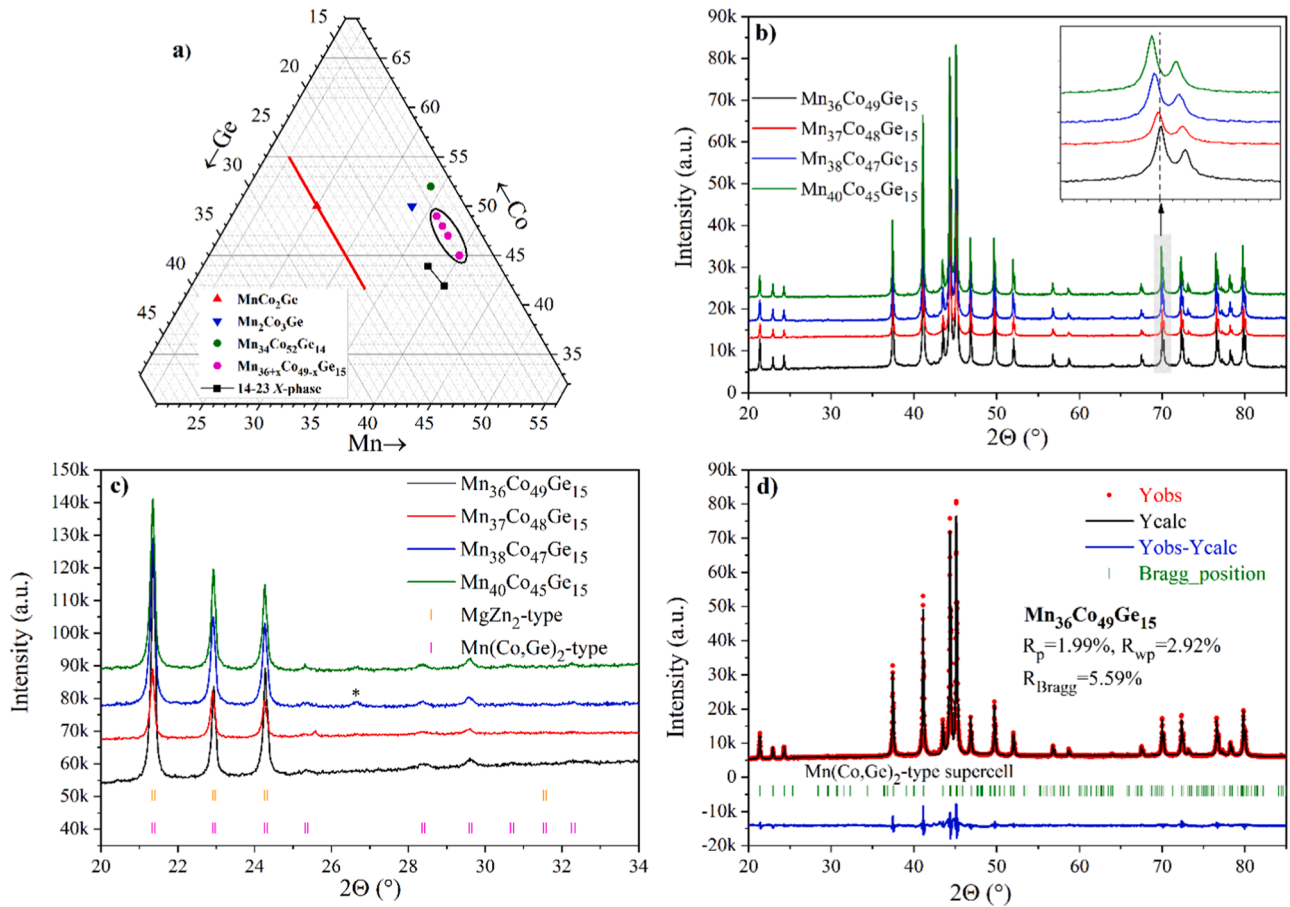


Fig. 2. a) Homogeneity regions of different phases along Ge isoconcentrate (Results for MnCo_2Ge and $\text{Mn}_2\text{Co}_3\text{Ge}$ were taken from literature [2], $\text{Mn}_{34}\text{Co}_{52}\text{Ge}_{14}$ [1] and $\text{Mn}_{14}(\text{Co},\text{Ge})_{23}$ [5]). b) XRD patterns for the $\text{Mn}_{36+x}\text{Co}_{49-x}\text{Ge}_{15}$ compounds (Inset shows peak shifts to lower 2θ -angle). c) Selected region of XRD patterns with an indication of weak superlattice peaks for all studied samples (this 2θ -region has been measured with 10 times longer exposure time to uncover weak superlattice peaks of the $\text{Mn}(\text{Co},\text{Ge})_2$ -type phase). The * is an unknown impurity. d) Rietveld refinement of the XRD-pattern for the $\text{Mn}_{36}\text{Co}_{49}\text{Ge}_{15}$ compound.

Table 1

Crystallographic parameters of the studied compounds with $\text{Mn}(\text{Co},\text{Ge})_2$ -type structure, $P6_3/mmc$ space group). Cell parameters for $\text{Mn}_{34}\text{Co}_{52}\text{Ge}_{14}$ [1] were recalculated in accordance with supercell settings.

Alloy	a (Å)	c (Å)	V (Å ³)	a (Å)	c (Å)	V (Å ³)	T_C (K)	T_{SRT} (K)
	XRPD			SCXRD				
$\text{Mn}_{34}\text{Co}_{52}\text{Ge}_{14}$	9.6005	7.7507	618.67	9.6058	7.7485	619.18	359	175
	(1)	(1)	(1)	(4)	(8)	(8)		
$\text{Mn}_{36}\text{Co}_{49}\text{Ge}_{15}$	9.6040	7.7531	619.31	9.589	7.742	616.5	330	187
	(1)	(1)	(1)	(4)	(3)	(5)		
$\text{Mn}_{37}\text{Co}_{48}\text{Ge}_{15}$	9.6062	7.7579	619.98	9.5076	7.6727	600.65	292	202
	(1)	(1)	(1)	(12)	(10)	(11)		
$\text{Mn}_{38}\text{Co}_{47}\text{Ge}_{15}$	9.6104	7.7591	620.62	9.6117	7.7590	620.78	251	203
	(1)	(1)	(1)	(6)	(4)	(6)		
$\text{Mn}_{40}\text{Co}_{45}\text{Ge}_{15}$	9.6152	7.7604	621.35	9.6413	7.7840	626.62	229	210
	(1)	(1)	(1)	(9)	(7)	(10)		

The natural question is how this can be understood. As indicated in a previous NPD study [3], the system has both antiferromagnetic and ferromagnetic interactions that are important to consider, and thus it is not possible to use crystallographic data presented in Table 1 to determine the strength of the exchange stiffness. Crystallographically, increasing the Mn content increases the unit cell volume as described above. This implies, ceteris paribus that on average the distance between the atoms increases. Concerning simpler binary Mn structures, the “Mn dilemma” [8] states that systems with short (<2.4 Å) Mn-Mn distances ($d(\text{Mn-Mn})$) tend to be nonmagnetic, intermediate (2.5–2.8 Å) tend to have small itinerant moments that couple antiferromagnetically, and

that systems with large $d(\text{Mn-Mn})$ (>2.9 Å) tend to favor ferromagnetism. The shortest $d(\text{Mn-Mn})$ in the present study vary from 2.8483(5) (for Mn1-Mn1, Mn1 is at 12k) and 2.9251(3) (for Mn1-Mn2, Mn2 is at 4f) Å ($x = 0$) to 2.8510(5) and 2.9285(3) Å ($x = 4$). As the $d(\text{Mn-Mn})$ are not changing enough to pass through the typical $d(\text{Mn-Mn})$ for nonmagnetic, itinerant magnetic moments, and ferromagnetism this indicates that the magnetic interaction types themselves are unaffected by the Mn content. In this sense, all the samples have the same types of magnetic interactions, although some of them are strengthened/weakened. As argued by Markin et al. [9], for $\text{Mn}_{1-x}\text{Co}_x\text{Ge}$ compounds increasing the Co content (or equivalently decreasing the

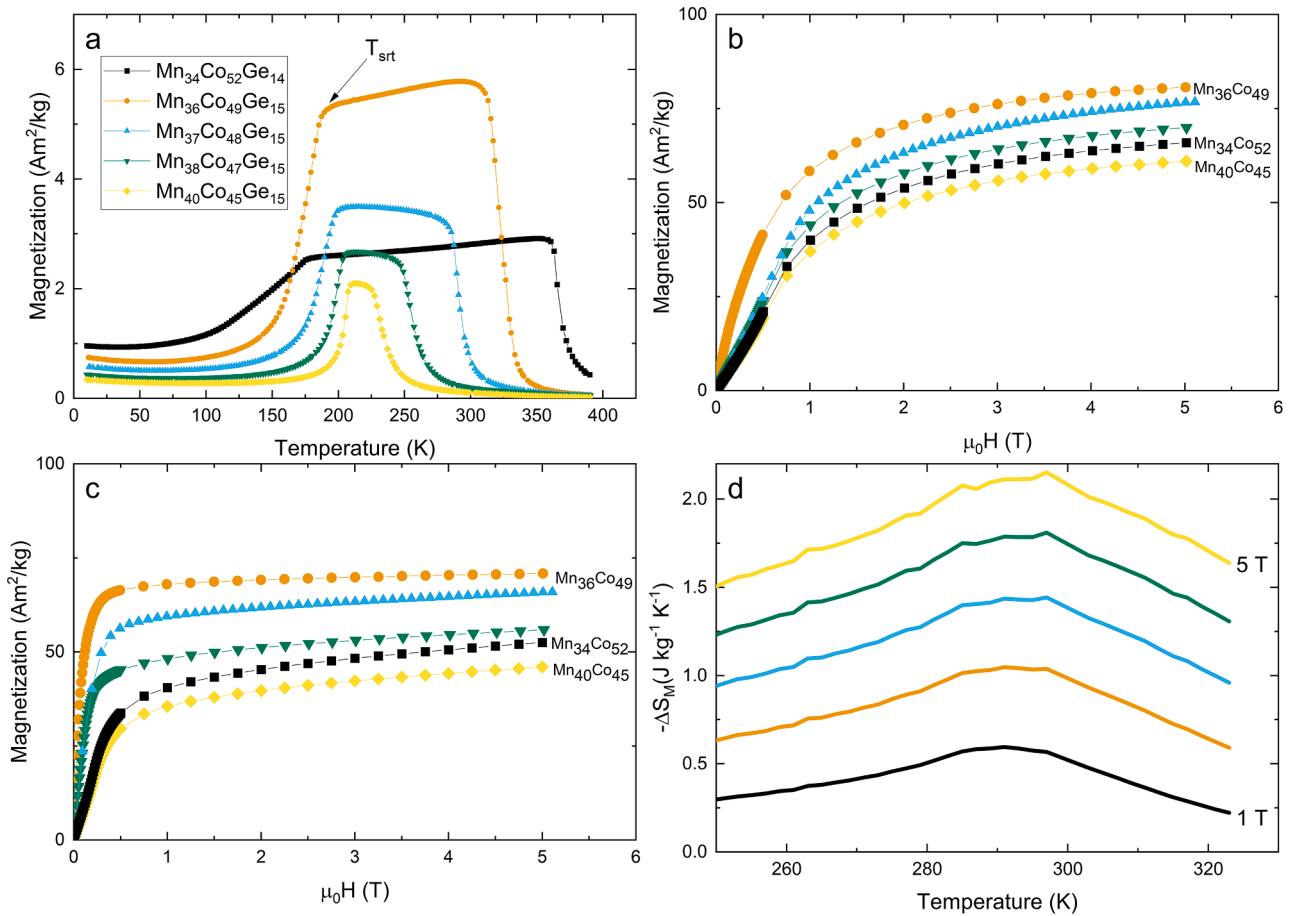


Fig. 3. a) Field cooled magnetization results in a magnetic field of 0.01T, b) magnetization versus field at 2 K, c) magnetization versus field at 200 K and d) isothermal magnetic entropy change for different magnetic fields.

Mn content) increases T_C for $1.2 \leq x \leq 1.4$ (the situation for other x is more complicated). This is the same trend for T_C is observed in the present study. Nawa et al. [10] studied the effect of nonstoichiometry in MnCo₂Si by computational methods and found that extra Mn changes T_C from 1050 K (Mn_{1.15}Co₂Si) to 1000 K (Mn_{1.44}Co₂Si). The nonstoichiometry also affected the magnetic moment, decreasing from 4.975 μ_B /f.u. (Mn_{1.15}Co₂Si) to 4.902 μ_B /f.u. (Mn_{1.44}Co₂Si). This is however a different ternary system, with a different structure, which may behave differently, but they showed that anti-site defects decrease the magnetic moment. In the present work, the extent of anti-site defects could not be quantified, but the NPD study [3] indicated that intermixing of Co and Mn is possible. The reduction of T_C is thus in line with results obtained for other similar systems and can be explained by strengthening of antiferromagnetic interactions as the Mn content is increased. The increase of T_{SRT} follows from this as at low temperature the system is antiferromagnetic [3].

At 2 K, samples are in the incommensurate antiferromagnetic state. Fig. 3b presents magnetization versus magnetic field curves at this temperature. These results are consistent with an incommensurate structure, with increasing magnetic field there is a spin-flop transition to a ferromagnetic state [3]. The magnetization in high enough magnetic field shows that the lowest Mn content has the highest magnetization. This reinforces the indication of increased antiferromagnetic interactions as the Mn content is increased. Referring to Fig. 3a at 200 K, the samples should be near or in the ferromagnetic region. The magnetization curves at 200 K as seen in Fig. 3c indicate that increasing the Mn content decreases the magnetization.

The T_C of Mn₃₇Co₄₈Ge₁₅ is close to room temperature. As this is a requisite for magnetocaloric materials operating at room temperature,

the potential as a magnetocaloric material was investigated. Fig. 3d shows the isothermal magnetic entropy change versus temperature using different magnetic fields H_f . The isothermal entropy change shows a maximum around 292 K, the T_C of this sample. This value is reaching 2 Jkg⁻¹K⁻¹ with $\mu_0 H_f = 5$ T, which can be compared to that of for instance Gd which reaches 10 Jkg⁻¹K⁻¹ with the same applied field. A more interesting view might be to compare it to other Mn–Co–Ge phases, which have been explored as magnetocaloric materials. Ma et al. [11] for example reported that varying the vanadium content in Mn_{1-x}V_xCoGe increases the isothermal entropy change from 1 Jkg⁻¹K⁻¹ to 9.5 Jkg⁻¹K⁻¹ under a magnetic field change of 1.2 T. Samanta et al. [12] reported that Mn_{1-x}Cu_xCoGe exhibits an isothermal entropy change of 53.5 Jkg⁻¹K⁻¹ for $x = 0.085$ and a field change of 5 T. Trung et al. [13] on the other hand reported on the properties of MnCoGeB_x and found 47.3 Jkg⁻¹K⁻¹ for MnCoGeB_{0.02}. The main difference between these materials and the Mn(Co,Ge)₂ presented in this study is that all the other materials are such that in addition to the magnetic transition there is a martensitic transformation from an orthorhombic TiNiSi-type structure to a hexagonal Ni₂In-type structure that drastically increases the isothermal entropy change. This indicate that the comparison to these materials, although interesting is somewhat misleading as the cause of the giant magnetocaloric effect in these systems is different as compared to the system studied here, as indicated by the results of [11–13].

In this work, we have synthesized samples of Mn(Co,Ge)₂ with composition Mn_{36+x}Co_{49-x}Ge₁₅ and established the homogeneity region to be $0 \leq x \leq 4$. Structurally, the larger atomic radius of Mn as compared to Co increases the lattice parameters and the accompanied volume. All samples show indications of superlattice peaks that are consistent with a doubling of the a and b lattice parameters as compared to the small cell

reported in [1]. Regarding magnetic properties, the main conclusions are that increasing the Mn content reduces T_C and increases T_{SRT} . The changes in T_C and T_{SRT} are accompanied with a reduction of the magnetization in the ferromagnetic and antiferromagnetic incommensurate regions, while in the incommensurate region the material experiences a spin-flop transition. The changes in T_C and T_{SRT} originate from increased antiferromagnetic interactions, consistent with the reduction of the magnetization.

The magnetic ordering temperature of $Mn_{37}Co_{48}Ge_{15}$ is $T_C = 292K$, therefore its potential as a magnetocaloric material was investigated. The investigation shows that the magnetocaloric effect is quite small, as the isothermal entropy change, using a magnetic field of 5T is $2Jkg^{-1}K^{-1}$. The isothermal entropy change is also small as compared to the giant magnetocaloric effect reported in other MnCoGe-based compounds, where accompanying the magnetic transition is a structural transition. Further advancement of $Mn(Co,Ge)_2$ as a magnetocaloric material needs to increase the magnetization while keeping T_C around room temperature. Introduction of non-magnetic elements, as those in $MnCoGeM_x$ ($M = B, Cu, \text{ or } V$) [11–13] may offer a promising route.

Declaration of Competing Interest

The authors declare that they have no known competing financial interests or personal relationships that could have appeared to influence the work reported in this paper.

Acknowledgement

Financial support from the Swedish Foundation for Strategic Research, project "SSF Magnetic materials for green energy technology" (EM16–0039) is acknowledged. We acknowledge Myfab Uppsala for providing facilities and experimental support. Myfab is funded by the Swedish Research Council (2019-00207). We thank Sagar Ghorai for

input on determination of magnetocaloric properties.

References

- [1] A. Vishina, D. Hedlund, V. Shtender, E.K. Delczeg-Czirjak, S.R. Larsen, O. Y. Vekilova, S. Huang, L. Vitos, P. Svedlindh, M. Sahlberg, O. Eriksson, H. C. Herper, Data-driven design of a new class of rare-earth free permanent magnets, *Acta Mater.* 212 (2021), 116913, <https://doi.org/10.1016/j.actamat.2021.116913>.
- [2] Y.B. Kuz'ma, E.I. Gladyshevskii, Crystal structure of the compound Mn_2Co_3Ge , *Dopovidi Akad. Nauk Ukr. RSR* 2 (1963) 205.
- [3] S.R. Larsen, V. Shtender, D. Hedlund, E.K. Delczeg-Czirjak, P. Beran, J. Cedervall, A. Vishina, T.C. Hansen, H.C. Herper, P. Svedlindh, O. Eriksson, M. Sahlberg, Revealing the Magnetic Structure and Properties of $Mn(Co,Ge)_2$, *Inorg. Chem.* 61 (2022) 17673–17681, <https://doi.org/10.1021/acs.inorgchem.2c02758>.
- [4] K.H.J. Buschow, P.G. Van Engen, R. Jongebreur, Magneto-optical properties of metallic ferromagnetic materials, *J. Magn. Magn. Mater.* 38 (1983) 1–22.
- [5] V. Shtender, S.R. Larsen, M. Sahlberg, Variants of the X-phase in the Mn–Co–Ge system, *Acta Crystallogr. Sect. C Struct. Chem.* 77 (2021) 176–180, <https://doi.org/10.1107/S2053229621002370>.
- [6] J. Rodriguez-Carvajal, Recent developments in the program FullProf, in *commission on powder diffraction (IUCr)*, Newsletter 26 (2001) 12–19.
- [7] W.B. Pearson, *The Crystal Chemistry and Physics of Metals and Alloys*, Wiley-Interscience, New York, 1972.
- [8] J.M.D. Coey, New permanent magnets; manganese compounds, *J. Phys. Condens. Matter.* 26 (2014) 64211.
- [9] P.E. Markin, N.V. Mushnikov, V.I. Khrabrov, M.A. Korotin, Magnetic properties of the $Mn_{1.9-x}Co_xGe$ compounds with a hexagonal crystal structure, *Phys. Met. Metallogr.* 106 (2008) 481–489, <https://doi.org/10.1134/S0031918X08110070>.
- [10] K. Nawa, I. Kurniawan, K. Masuda, Y. Miura, C.E. Patrick, J.B. Staunton, Temperature-dependent spin polarization of Heusler Co_2MnSi from the disordered local-moment approach: effects of atomic disordering and nonstoichiometry, *Phys. Rev. B* 102 (2020), 054424, <https://doi.org/10.1103/PhysRevB.102.054424>.
- [11] S.C. Ma, Y.X. Zheng, H.C. Xuan, L.J. Shen, Q.Q. Cao, D.H. Wang, Z.C. Zhong, Y. W. Du, Large roomtemperature magnetocaloric effect with negligible magnetic hysteresis losses in $Mn_{1-x}V_xCoGe$ alloys, *J. Magn. Magn. Mater.* 324 (2012) 135–139, <https://doi.org/10.1016/j.jmmm.2011.07.047>.
- [12] T. Samanta, I. Dubenko, A. Quetz, S. Stadler, N. Ali, Giant magnetocaloric effects near room temperature in $Mn_{1-x}Cu_xCoGe$, *Appl. Phys. Lett.* 101 (2012), 242405, <https://doi.org/10.1063/1.4770379>.
- [13] N.T. Trung, L. Zhang, L. Caron, K.H.J. Buschow, E. Brück, Giant magnetocaloric effects by tailoring the phase transitions, *Appl. Phys. Lett.* 96 (2010), 172504, <https://doi.org/10.1063/1.3399773>.